

A Rapid Electrochemical Impedance Spectroscopy and Sensor-Based Method for Monitoring Freeze-Damage in Tangerines

Pablo Albelda Aparisi^{ID}, Elena Fortes Sánchez^{ID}, Laura Contat Rodrigo^{ID},
Rafael Masot Peris^{ID}, and Nicolás Laguarda-Miró^{ID}

Abstract—This study focuses on the analysis and early detection of freeze-damage in tangerines using a specific double-needle sensor and Electrochemical Impedance Spectroscopy (EIS). Freeze damage may appear in citrus fruits both in the field and in postharvest processes resulting in quality loss and a difficult commercialization of the fruit. EIS has been used to test a set of homogeneous tangerine samples both fresh and later frozen to analyze electrochemical and biological differences. A double-needle electrode associated to a specifically designed electronic device and software has been designed and used to send an AC electric sinusoidal signal 1 V in amplitude and frequency range [100Hz to 1MHz] to the analyzed samples and then receive the electrochemical impedance response. EIS measurements lead to distinct values of both impedance module and phase of fresh and frozen samples over a wide frequency range. Statistical treatment of the received data set by Principal Components Analysis (PCA) and Partial Least Squares Discriminant Analysis (PLS-DA) shows a clear classification of the samples depending on the experienced freeze phenomenon, with high sensitivity (1.00), specificity (≥ 0.95) and confidence level (95%). Later Artificial Neural Networks (ANN) analysis based on 20-3-1 architecture has allowed to create a mathematical prediction model able to correctly classify 100% of the analyzed samples (CCR =100% for training, validation and test phases, and overall classification), being fast, easy, robust and reliable, and an interesting alternative method to the traditional laboratory analyses.

Index Terms—Double-needle sensor, electrode, electrochemical impedance spectroscopy (EIS), tangerine, freeze damage, detection, artificial neural networks (ANN).



I. INTRODUCTION

TANGERINE (*Citrus reticulata*) is the second most produced citrus variety in the world (33,414 thousand tons),

Manuscript received January 21, 2021; revised February 10, 2021; accepted March 8, 2021. Date of publication March 12, 2021; date of current version April 16, 2021. This work was supported by the Spanish Government/FEDER funds [Ministerio de Economía y Empresa (MINECO)/Fondo Europeo de Desarrollo Regional (FEDER)] under Grant RTI2018-100910-B-C43 and in part by the Conselleria d'Educació, Investigació, Cultura i Esport de la Generalitat Valenciana under Grant GV/2018/090. The associate editor coordinating the review of this article and approving it for publication was Prof. Venkat R. Bhethanabotla. (Corresponding author: Nicolás Laguarda-Miró.)

Pablo Albelda Aparisi and Elena Fortes Sánchez are with the School of Design Engineering, Universitat Politècnica de València, 46022 Valencia, Spain (e-mail: pabalap@etsid.upv.es; elforsan@etsid.upv.es).

Laura Contat Rodrigo, Rafael Masot Peris, and Nicolás Laguarda-Miró are with the Interuniversity Institute of Molecular Recognition and Technological Development (IDM), Universitat Politècnica de València, 46022 Valencia, Spain (e-mail: lcontat@ter.upv.es; ramape@eln.upv.es; nilami@iqn.upv.es).

Digital Object Identifier 10.1109/JSEN.2021.3065846

only behind orange production (73,313 thousand tons) and far away of lemons and other citrus varieties, representing 22.8% of total citrus production [1], [2]. Spain (1,967 thousand tons) is the first tangerine producer country in the Mediterranean region, only behind China which is the first world power in the sector with 19,000 thousand tons. On the other hand, in terms of exports, Spain is a world leader, dedicating 1,367 thousand tons to international marketing, almost 70% of its annual production. Therefore, this is a sector in which cultivation, harvesting, post-harvest and commercialization are of capital importance for the country.

Cultivation and postharvest of tangerines, as oranges [3] and lemons [4], have a serious problem with freeze-damage [5], [6], despite their different cultivar characteristics [7]. Cold winter nights when temperature drops below freezing may affect the fruit. Furthermore, inadequate management of the refrigerated storage and transport of these fruits can also lead to freezing and quality loss of the fruits [8]. This can occur

TABLE I
REPORTED METHODS FOR FREEZE DAMAGE
DETECTION IN CITRUS FRUITS

Technique	Analyte	Fruit	Reference
Visual inspection	Segment walls, pulp	Citrus fruits	[19]
Flotation separation	Specific gravity	Marsh	[20]
		grapefruits, citrus fruits	[21]
Vis/SWNIR spectroscopy	Half-transmittance	Sweet lemons	[22]
Gas sensors	CO ₂ , ethanol	Valencia oranges	[23]
Electronic nose	Overall gas profile	Valencia oranges	[23]
GC-MS	Volatile emissions	Navel oranges	[24]
UV fluorescence	Peel oil constituents	Navel oranges	[25]
NMR spectrometry	Proton spin-spin relaxation time	Navel oranges	[26]
EIS	Impedance	Navelate oranges,	[3]
		lemons	[4]

if the fruits reach temperatures below -1.7°C to -2.8°C [9]. Intensity and duration of the frost, variety, maturity and other bioclimatic factors influence the severity of the freeze-damage in the fruits [10], [11]. If it is rapid, which can occur in a poorly regulated container, ice crystals will break the cell wall as they form both outside and inside the cells, without time for any adaptation. Then, cell death (necrosis) appears and the impossibility of tissue recovery. Consequently, the fruit becomes unsuitable for normal marketing [12]. Conversely, if freezing occurs slowly enough, initial freezing of the interstitial fluid may allow a progressive osmotic balance between the liquids inside and outside the cells. If this process and the subsequent thawing are not too demanding for the cells, they can recover without further damage [4].

Some of the physical and metabolic effects of chilling in tangerines are scald or oil-gland darkening and pitting [13], necrosis, rind staining [14], red blotches and watering breakdown on the flavedo [15], and internal drying [16]. The particular problem of these effects is that some of them are neither immediate nor obvious, so chilling injuries are sometimes difficult to identify.

Fortunately, advances in research and technology have allowed quality control methods to evolve and improve [17] and, focusing on the aim of this study, those devoted to freeze damage by sensing [18]. Specifically, several methods have been developed to identify freezing damage in citrus fruit (table I) ranging from observation of the fruit [19] and physical techniques such as separation by flotation [20], [21] to the use of vision sensors [22] and other laboratory methods like ethanol detection [23], gas chromatography/mass spectroscopy (GC/MS) [24], fluorescence [25] or nuclear magnetic resonance [26]. Most of these methods are complex, expensive, and time-consuming and they are only carried out by specialized laboratories and personnel.

By contrast, EIS is revealing as a fast, easy-to-use, inexpensive, and reliable technique [27]. Once it is implemented, no specialized personnel or complex laboratory equipment is needed so it can be used directly on-site for measurements in field or in the agri-food industry [28]. Essentially, EIS

consists in the electrical characterization of a material by means of sensors and the association of the electrical response to certain parameters of the material [29]. EIS is already being used in agri-food industry for quality control of products [30] like vegetables such as potatoes [31], carrots [32], [33], eggplants [34] and tomatoes [35], some fruits like kiwis [36], bananas [37] and mangoes [38], meat [39], [40] and fish [27], honey [41] processed products [42] and the valorization of agri-food wastes [43], [44].

Nowadays, the evolution of computer systems allows the use of significant amounts of information in statistical data-processing [45]. Thus, specific statistical software allows us to carry out complex analyses of the electrical responses of EIS tests [46]. In this sense, PCA and PLS analyses [47]–[49] and even Artificial Neural Networks modelling [50], [51] can be conducted in a fast and reliable way. ANNs, due to their characteristics (flexibility, adaptability, and easy fitting to non-linear systems) [52], are powerful tools for this type of applications [53], [54]. They allow obtaining relatively simple, self-corrective and self-learning mathematical models, easily implementable in a microprocessor, being particularly reliable, and robust [55], [56]. Thus, ANNs are ideal for detecting electrochemical changes in agri-food products and their correlation with variations in specific quality parameters [57].

The objective of the present study is to develop a methodology based on the combination of EIS and Artificial Neural Networks for a rapid, economic, and reliable freeze-damage detection in tangerines.

II. MATERIALS AND METHODS

A. Selection and Preparation of the Samples

Tangerines cv. ‘Clemenvilla’ (Citrus reticulata Hort. ex Tanaka) were purchased from a local market choosing those as similar as possible (same cultivar, origin and batch, caliber, physical aspect, ripeness. . .) in order to assure homogeneity in the set [51]. Once in the laboratory, a set of 10 tangerines was selected, washed, dried and stored at room temperature for at least 12 hours for fruit tempering.

For post-freezing assays, the selected samples were introduced in a freezer (LIEBHERR Model GGU 1500 Premium, Liebherr- International Deutschland GmbH, Biberach an der Riß, Germany) time enough to reach the freezing temperature of the fruit, simulating the effect of a chilling night. Samples were then stored in the laboratory at room temperature for 12 hours to be tempered again and proceed with the corresponding assays.

B. Electrochemical Impedance Spectroscopy

EIS was the selected technique to carry out the assays as it is showing promising results in several fields and particularly in agri-food applications [30]. This technique consists of a) applying a sinusoidal voltage for a certain frequency between two electrodes inserted in a sample, b) measuring the electrical intensity between them, that is, the current through the sample and finally, c) obtaining the impedance for the established frequency by means of the voltage and current values. Then, the process is repeated for another frequency

TABLE II
SPECIFICATIONS OF THE DESIGNED EIS DEVICE

Parameter	Specifications
Signal amplitude	0mV-500mV
Frequency range	1Hz-1MHz
Type of signal	Sinusoidal
Measured Parameters	Current and Voltage
Impedance calculation	Discrete Fourier Transform
Output Data	Impedance Modules and Phase
Data per assay	100 data (50 for modules and 50 for phases)

and so on within a determined frequency range, obtaining the impedance spectrum of the studied sample. Impedance will depend on the properties of the material so differences in the received signals can be associated with specific changes in the samples [58].

There are several electronic systems able to provide the impedance spectrum of a sample, such as those referred by Wu *et al.* [34], Rehman *et al.* [59], Juansah *et al.* [60], Ando *et al.* [61], Ando *et al.* [32], Ando *et al.* [62], Imaizumi *et al.* [63], Chowdhury *et al.* [37], Tian-Hao Chen *et al.* [64] and Lima *et al.* [65]. In order to gain in versatility most of these commercial systems are expensive and large devices, compared to the one introduced in this paper.

On the contrary, the applied EIS system was designed by the Group of Electronic Development and Printed Sensors (GED+PS), a research group inside the Interuniversity Institute for Molecular Recognition and Technological Development (IDM) at the Universitat Politècnica de València (UPV). The system consists of an electronic device and a software application to be run in a computer [66] and has been particularly designed and optimized to obtain the impedance spectrum of food samples.

C. Electronic Device

The designed hardware is able to generate sinusoidal voltage signals in specific frequency [1Hz to 1MHz] and amplitude [−0.5V to +0.5V] ranges and receive the corresponding current responses to generate EIS datasets according to the specifications described in table II.

In order to do so, the device is connected to a personal computer (PC) or laptop via USB port and consists of two complex programmable logic devices (CPLD, Altera EPM7160SLC84). The first CPLD, associated with a 10-bit digital-analogue converter (DAC) and a static 2KB (2048bytes) random access memory (RAM), is devoted to receiving the process data from the software in the PC. The second one, with two 8-bit analogue-digital converters (ADC), several analogue signal adaption circuits and a configurable current sensor, is programmed to sample the signals corresponding to both the applied voltage and the received current response [29] (fig. 1).

A specifically designed sensor allowed both applying and measuring voltage and current. This sensor consists of a couple of parallel stainless-steel needles (electrodes) 1,5 cm in length and 1 mm in diameter. The needles were fixed in an epoxy cylinder to ensure a constant distance of 1 cm between the

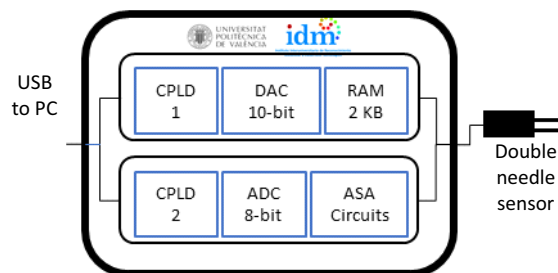


Fig. 1. Scheme of the designed EIS Device and sensor.



Fig. 2. The stainless-steel double-needle sensor.

electrodes as well as the necessary resistance and durability of the sensor (fig. 2).

D. Software Application

The software was designed to be easily configurable by the user. It is able to generate the defined electric signal (frequency sweep and amplitude) and send the commands for its application via the USB port of the PC to the electronic device that generates the sinusoidal waveform.

The sampled current and voltage signals are sent to the PC. Then, the software uses the data and a discrete Fourier transform (DFT) to determine amplitude and phase for both voltage and current signals. Then, the corresponding impedance (module and phase) of the sample for each one of the analyzed frequencies is calculated and stored. The system is able to sample up to 100 data (50 for modules and 50 for phases) per assay.

E. Cryo-Field Emission Scanning Electron Microscopy

Morphology and microstructural changes in the samples were studied by Cryo-FESEM on a microscope ZEISS ULTRA 55 (Oxford Instruments, Abingdon, UK) in the Electron Microscopy Service at the UPV.

Firstly, samples were prepared and mounted on a sample holder, in order to be frozen in slush nitrogen and transferred to a preparation chamber. Then, samples were fractured, sublimated for 10 minutes at −90 celsius degrees to reveal the inner structure and coated with platinum for 15 seconds. Finally, they were introduced in the microscope chamber to be observed. Imaging conditions were 2 kV acceleration voltage and 5 mm working distance (WD).

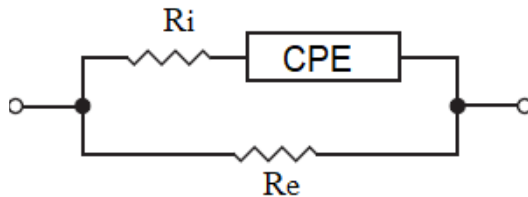


Fig. 3. The electrical equivalent circuit (modified Hayden model).

F. EIS Analyses

After selection and preparation of the samples, the fruits were analyzed in the following ways, introducing the sensor a) directly into the peel, b) into a section of the fruit without the peel, and c) between two sections trying to keep the membrane between sections in the middle of the electrodes. These three different sets of assays were designed to let us know which part of the tangerine changed its electrochemical properties in a more remarkable way. In other words, these assays would discriminate the most sensitive part of the tangerines to freeze. Additionally, each test was repeated in three different parts of the sample, with three iterations per test summing up a total of 27 dataset per fruit. As each sample was tested twice (fresh and frozen), and each data set consisted of 100 data (50 module and 50 phase values), up to 5400 values per tangerine were obtained for an overall studied dataset of 54.000 values.

Assays were carried out following a previously defined test-protocol: First, the complete EIS-measuring system was checked to assure it was well connected and then turned on. Afterwards, the conditions of the assay to be performed were designed by introducing the appropriate instructions into the software. Next, the sample to be analyzed was attached to a specific support and temperature was measured by using a multimeter (FLUKE 16 Multimeter, FLUKE, Everett, WA, USA). Then, the corresponding sample was punctured with the sensor and the measurement started by generating the previously defined electric wave. The connection wire transmitted the signal to the sensor and it was in charge to transmit it into the sample between the electrodes and also receive the response that was immediately showed in the PC screen and stored as a dataset for further data treatment.

G. Data Treatment

An appropriate data treatment was required as the response signal for each assay consisted of 100 data (50 module data and 50 phase data) resulting in an overall data set both large in volume and complex in interpretation. Data preprocessing was carried out by Exponential Smoothing [66]. This technique was used as a filter in order to reduce noise in the obtained raw EIS data.

Then, the EIS dataset was analyzed using an equivalent circuit model. To do this, the modified Hayden model was selected as it shows a better fit to the EIS of biological tissues than other simpler models as those proposed by Cole and Hayden [62] (fig. 3). Essentially, CPE is conceived as a combination of resistances and capacitors or as an imperfect capacitor [32] able to explain the inhomogeneous distribution of cells in the biological tissues [63].

Proteus©software (Labcenter Electronics, North Yorkshire, England) and the Generalized Reduced Gradient (GRG) non-linear algorithm (Excel Solver) were used to both determine the different parameters of the equivalent circuit and fit the model with the experimental EIS data.

Next, a double statistical, data treatment was performed: first, a multivariate data analysis was carried out both in a non-supervised and supervised analysis via PCA and PLS-DA and then an ANN analysis to model the freeze phenomenon in the samples. Multivariate data treatment was conducted by using the software SOLO©(Eigenvector Research, Ind., Manson, WA, USA). These analyses were performed in a double way. First, a PCA was carried out in order identify natural aggrupation of samples and try to correlate groupings with some particularity of the samples (e.g. having experienced a freeze phenomenon). Then, a PLS-DA was conducted in order to discriminate samples attending to the studied variables and find out significant differences, as this type of regression analysis has a dependent variable that is categorical (the class to which samples belong) and several numerical independent variables [67], [68]. In PLS-DA analyses, these independent variables were new and were obtained systematically from the original ones: 100 data per assay (50 modules and 50 phases). In order to conduct these PLS-DA analyses, the original data set was divided as follows: 67% of the data were used for calibration and the remaining 33% were devoted to test the obtained model [69]. Data pre-processing was conducted by auto-scale (standardization and mean centering). Additionally, Venetian blinds were used for cross-validation. Robustness and validity of the obtained models were analyzed by the coefficient of determination (R^2) and the root mean square errors for cross validations (RMSCV) and prediction (RMSEP).

Attending to the particularities of the samples in this study, being natural in origin and potentially affected in terms of electrochemical response by several variables (size, ripeness, temperature, acidity, sugar content...) an alternative data treatment analysis was conducted by ANNs. This type of networks is of interest as the obtained models are flexible, adaptative, easy to program and use, easy fitting to non-linear systems, self-learning and low in computational requirements [52, 53]. Additionally, these networks are already successfully used with complex and variable data sets to implement easy, low demanding, adaptative and reliable models in microprocessors for multiple purposes by using simplified ANNs.

ANN analyses were carried out by using the software Alyuda Neurointelligence 2.2 ©(Alyuda Research Inc., Cupertino, CA, USA). To do so, the obtained EIS data were randomly divided into three different sets in order to conduct the network training (70% of the data) and proceed with the model validation (15%) and test (15%). The training phase allowed the design of the appropriate ANN model while validation and test phases assessed the soundness of the selected model by using previously used and independent data, respectively. A series of preliminary trials helped to select the type and structure of the ANN thus designing the essentials of the network architecture. Then, a more in-depth study allowed to set the details of the selected ANN (layers and number of neurons in each layer, neuron functions and functions to work

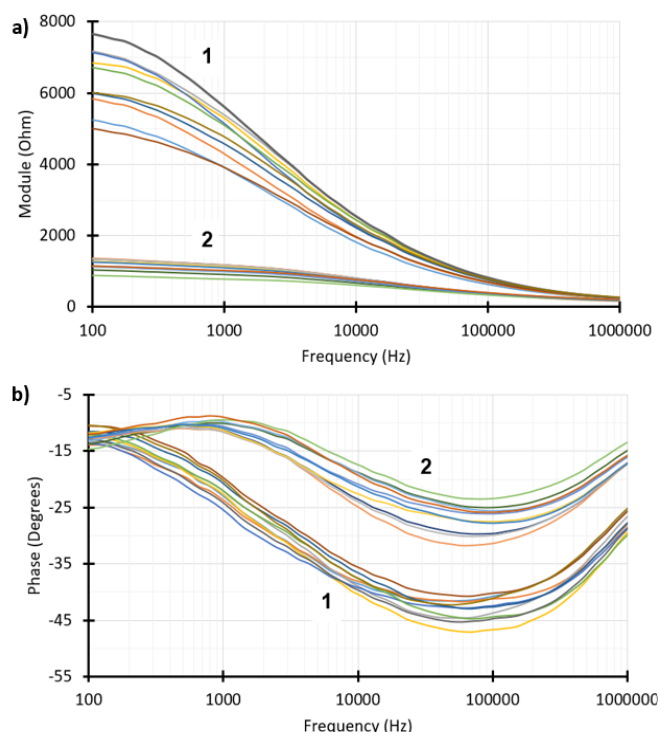


Fig. 4. Averaged a) Module and b) Phase of the EIS results for tangerines both fresh (1) and frozen (2) punctured between two sections.

within the layers) thus being the selected ANN completely defined.

The handicap of overfitting ANN-based prediction models was avoided by using a proportional structure of the network, cross-validation, and early stopping. Finally, accuracy and robustness of the obtained neural prediction model were expressed by the correct classification rate (CCR%) and the confusion matrix (clearly showing success in the prediction process by indicating hits and mistakes in the samples classification).

III. RESULTS AND DISCUSSION

A. EIS Results

Electrochemical responses to the conducted EIS assays in the fruit samples composed a set of 50 modules and 50 phase values per assay for an overall of 54,000 dataset (100 data/assay, 10 samples, 2 freeze exposure conditions/sample, 3 different types of assay/sample, 3 repetitions/assay, and 3 iterations/repetition). The obtained values were appropriately sampled in the PC and represented in a graphical interface as shown in fig. 4.

Figure 4a shows a trend to separation between modules of fresh samples and those previously frozen. This trend is particularly clear in frequencies in the range [100Hz to 1kHz] being modules in the higher part of the figure corresponding to fresh fruits and the ones in the lower those corresponding to the frozen samples. Looking at the phases (fig. 4b), the opposite behavior is observed: phases remain quite mixed in the lower frequency ranges and become more clearly separated depending on freezing exposure in the middle frequencies of the analyzed range [1kHz to 100kHz]. In this case, phases for

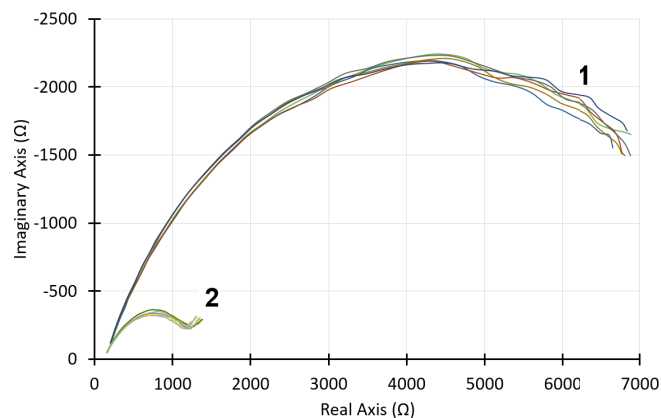


Fig. 5. Nyquist diagram of the averaged EIS results for tangerines both fresh (1) and frozen (2).

the fresh samples are in the lower part of the graphic and those belonging to frozen fruit samples are in the higher part.

Nyquist diagrams were also available in the graphic interface of the software providing graphical plots of both real and imaginary parts of the impedance in a determined frequency range. For the specific case of EIS analyses for tangerine n^o4 punctured between two sections in the range [100Hz to 1 MHz] the Nyquist diagram was as shown in figure 5.

This figure shows how the capacitive component (the imaginary part of the impedance) of the frozen samples (2) is remarkably lower than the one of the fresh samples (1). This is due to the freeze/thaw process altering the cells and thus the biological tissue provoking cell shrinkage and liquid loss, vacuole membrane breakdown and cell wall dissolution, ion leakage to the intercellular liquid and, in terms of biologic tissue, cell separation and larger intercellular spaces [18], [70].

Specifically, Nyquist plots in the studied frequency range [100kHz-1MHz] allow to analyze changes in the cell membranes as this frequency correspond to the β dispersion area [71] in which polarization of proteins, organic macromolecules and other elements constitutive of the cell membranes occur [72]. Thus, it is possible to identify fresh and frozen tangerine samples as freeze-damage alters the cell wall and inner cell membranes that are those electrically acting as capacitors in the electrical equivalent circuit (fig. 2). The affection to the cells and the overall biological tissue decreases their capacitive ability and, therefore, their impedance, showing a different electric behavior (fig. 5).

B. Cryo-FESEM Results

It has been reported that the extent of freeze-damage in fruit tissue is related to the distribution and the size of crystals, which are determined by the freezing rate. Cryo-FESEM was used to investigate the microstructure of fresh and frozen tangerine tissues. The bright regions in the micrographs correspond to the freeze concentrated matrix, the cytoplasmic membrane and the cell walls, whereas the darker regions correspond to the ghost of ice microcrystals that sublimed during etching.

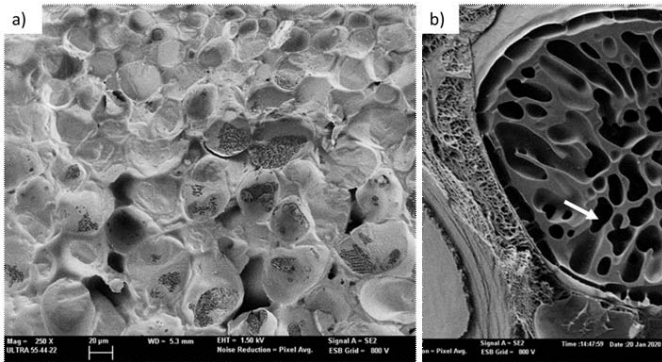


Fig. 6. Cryo-FESEM images of a) fresh and b) frozen at $-1.5\text{ }^{\circ}\text{C}$ tangerine tissue. Ice crystals are arrowed. (a) scale bar = 20 μm and (b) scale bar = 2 mm).

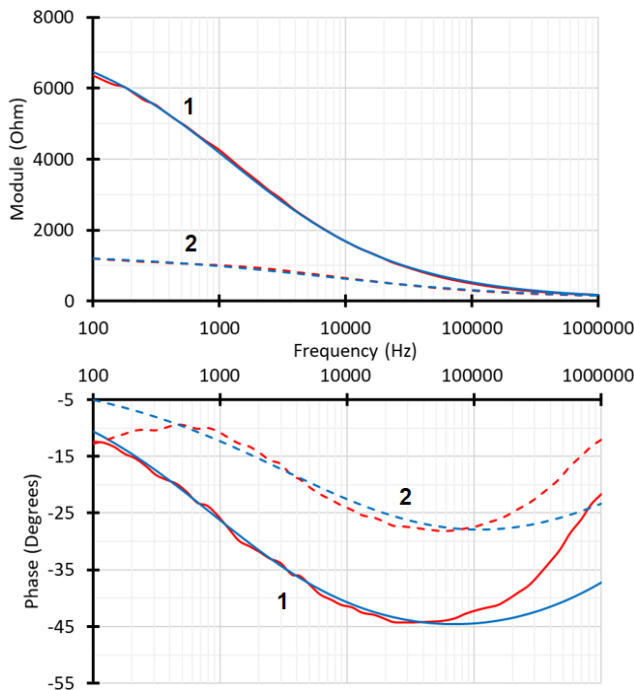


Fig. 7. The electrical equivalent model fitting with the experimental a) Module and b) Phase EIS results for tangerines both fresh (1) and frozen (2).

The tissue of fresh samples is composed of uniformly distributed cells, and the cell walls appear intact and with no sign of damage (fig. 6a). The appearance of frozen samples is shown in figure 6b. The sublimation of the ice crystals formed during freezing reveals the fingerprint of the microcrystals' sizes and shapes. As expected, slow freezing at $-1.5\text{ }^{\circ}\text{C}$ induces the formation of large ice crystals. Furthermore, the cell walls seem to be less regular after freezing.

C. Data Treatment Results

Similarly, the complete data set (module and phase data in the complete frequency range) was used to carry out the data treatment.

Firstly, an analysis of the obtained EIS data was performed. Figure 7 shows the results of fitting the theoretical model with the experimental data for tangerines both natural and frozen

TABLE III
CHARACTERIZATION OF THE OBTAINED ELECTRIC EQUIVALENT MODEL

Type of Tangerine	Electrical parameters	Fitting parameters
Fresh	$\alpha=0.5732$	$R^2(\text{module})=0.9996$
	$\text{CPE}=9.07\text{E-}7\text{F}$	$\text{RMSE}(\text{module})=38.5324\Omega$
	$R_i=53.4773\Omega$	$R^2(\text{phase})=0.8484$
	$R_e=7721.8984\Omega$	$\text{RMSE}(\text{phase})=4.5634^{\circ}$
Frozen	$\alpha=0.479$	$R^2(\text{module})=0.9959$
	$\text{CPE}=4.95\text{E-}6\text{F}$	$\text{RMSE}(\text{module})=22.6126\Omega$
	$R_i=73.4067\Omega$	$R^2(\text{phase})=0.7630$
	$R_e=1340.0689\Omega$	$\text{RMSE}(\text{phase})=3.9337^{\circ}$

TABLE IV
PCA COMPARISON RESULTS. CUMULATIVE PERCENTAGE OF THE VARIANCE

Type of Assay	Number of principal components		
	1	2	3
Peel	73.72%	90.67%	95.67%
Without the peel	67.09%	84.58%	96.04%
Between two sections	73.50%	93.12%	96.62%

punctured between two sections. The ability of the model to fit with the experimental data in the frequency range [1kHz to 100kHz] is particularly remarkable.

The electrical parameters of the designed electrical equivalent model and the goodness of its fitting with the experimental data are shown in Table III. In the resistive part of the model, an increase in the R_i value and the corresponding decrease of R_e can be seen when freezing and thawing occurs. Correspondingly, a decrease in α , and CPE values is observed. All these changes in the electrical parameters are directly linked to the physical-chemical and biological alterations experienced by the samples' tissues when freezing, as explained in section III.A.

Next, a PCA comparison was carried out with the obtained EIS results in order to guess if there was a clear separation of the data depending on their electrochemical response. The results showed a) a clear separation of the samples depending on whether they were fresh or frozen and b) a slightly better differentiation for assays conducted between two sections of the tangerines (see table IV). Thus, the data set corresponding to this type of assays was the one selected for further statistical analyses and artificial neural network modeling.

Figure 8 shows the graphical representation of the conducted PCA analysis with the results of the analyses carried out between two sections. As observed, 73,50% of the variance was explained with just one principal component and an additional 19,63% done with the second one summing up an overall 93.13% of the variance explained with just two principal components.

Afterwards, a PLS-DA analysis was carried out. The goal was to confirm that classifying the samples into two different classes (fresh vs frozen samples) was possible by means of an appropriate mathematical model. The results of the PLS analysis, shown in figure 9, confirmed that it was possible with a high sensitivity and specificity of the proposed model. The graphical representation confirms these terms as there is a

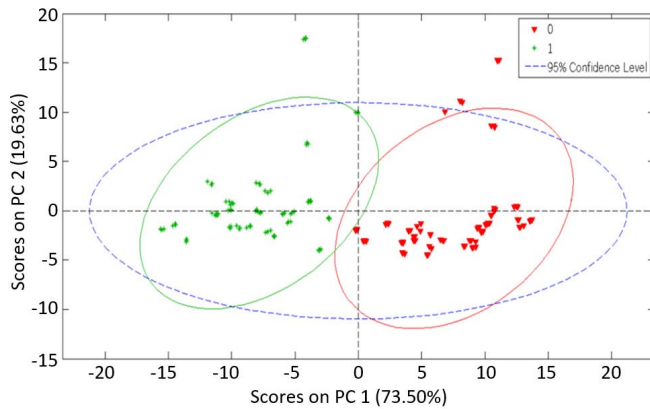


Fig. 8. PCA analysis of EIS tests conducted between two sections of the analyzed fresh tangerine samples (in green) and frozen samples (in red).

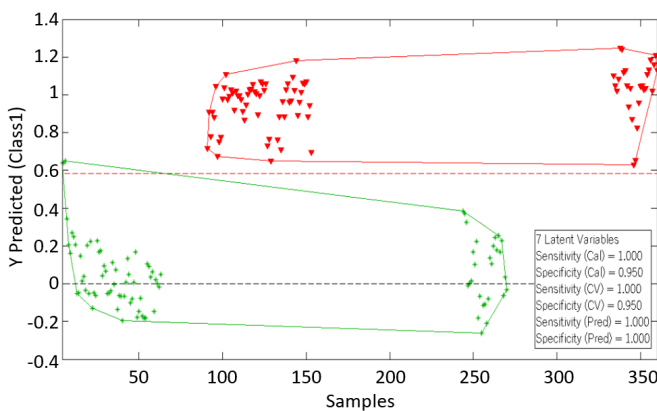


Fig. 9. PLS-DA analysis of EIS tests conducted between two sections of the analyzed fresh tangerine samples (in green) and frozen samples (in red).

clear separation among samples: those corresponding to frozen samples (in red) were placed in the upper side of the graphic as those from fresh ones (in green) were located in the lower side with no intersection area between these two groups.

D. ANN Results

Additionally, an ANN study was carried out to analyze if freeze-damage prediction by EIS improved when using a more flexible adaptive and non-linear model method. In a preliminary approach, it was observed that freeze-damage detection in tangerines was possible with relatively simple ANN structures. To do so, different ANN architectures were tested by using the search architecture function of the Alyuda Neurointelligence 2.2 ©software and the best ones were selected according to their fitness. Different combinations of algorithm training functions (quick propagation, conjugate gradient descent and on-line back propagation) and node activation functions (linear, logistic and hyperbolic tangent) were considered.

Then, in a more in-depth analysis EIS data were analyzed and randomly divided in datasets for training (70%), validation (15%) and test stages (15%), and appropriately pretreated (normalized). An 20-3-1 architecture was selected as the best of the possible studied architectures attending to its number of weights, fitness, and train, validation and test errors.

TABLE V
CCRs AND CONFUSION MATRICES FOR THE OBTAINED ANN MODEL FOR TANGERINE FREEZE-DAMAGE DETECTION

		ANN ARCHITECTURE: 20-3-1							
		TRAINING		VALIDATION		TEST		TOTAL	
		TARGET CLASS							
		1	0	1	0	1	0	1	0
OUTPUT CLASS	1	60	0	12	0	12	0	84	0
	0	0	60	0	15	0	15	0	90
		60	60	12	15	12	15	84	90
		0	0	0	0	0	0	0	0
		100%	100%	100%	100%	100%	100%	100%	100%

The selected 20-3-1 network was a three-layer pyramidal structure with 20 nodes in the input layer, three hidden-nodes in the intermediate layer and just one output node. The selected algorithm to train the network was on-line back propagation with hyperbolic tangent type functions as activation functions in both the hidden-layer nodes and the output node as this combination showed the best accuracy. Then, the network was trained, validated, and tested by iterations. Correct classification rates (CCRs), confusion matrices and error dependence plots were easily obtained with the software and were used to assess the suitability of the studied ANN. The obtained network demonstrated to be very effective in discriminating tangerine samples depending on they had experienced a freeze phenomenon or not, showing excellent correct classification rates (CCRs) and no network errors for training, validation and test phases and in the overall classification of the studied samples (table V).

Results reveal that freeze-damage in tangerines can be early detected by means of the presented EIS-based method with a double-needle stainless steel electrode and the use of ANN analyses for data treatment.

IV. CONCLUSION

Freeze-damage control is fundamental for early detection of quality loss in agri-food products and improve the decision making in order to minimize wastes and decide alternative uses for those products not fitting with the standards to be commercialized. It becomes of essential importance for fruits like tangerines being freeze-sensitive and the second most commercialized citrus fruit in the world.

The performed EIS analyses have proved to be effective in freeze-damage detection in tangerines. EIS results allow for clear distinction between both the modules and the phase of the impedance of the fresh and frozen samples over a wide frequency range. When EIS results were combined with PLS-based data treatment, the obtained model showed high specificities (≥ 0.95) and sensitivities (1.00) for calibration, validation and test phases, but it was particularly remarkable when combined with ANN-based prediction models. The ANN-based method demonstrated very high accuracy, reliability and robustness being able to correctly classify 100% of the analyzed samples (CCR = 100%), discriminating those fresh and those having experienced a freeze-phenomenon.

The obtained results allow to introduce the EIS-based techniques as promissory methods for specific quality control processes in fruits and particularly for early freeze-damage detection in tangerines. Additionally, these types of techniques are easy-to-use, rapid, inexpensive and reliable, overcoming other laboratory techniques.

REFERENCES

- [1] FAOSTAT. (2019). *Food and Agriculture Data*. Accessed: Dec. 30, 2019. [Online]. Available: <http://www.fao.org/faostat/en/#data>
- [2] *Citrus Fruit Fresh and Processed Statistical Bulletin 2016*, Food Agricult. Org., Rome, Italy, 2017, p. 66.
- [3] E. Serrano-Pallicer, M. Muñoz-Albero, C. Pérez-Fuster, R. M. Peris, and N. Laguarda-Miró, "Early detection of freeze damage in navelate oranges with electrochemical impedance spectroscopy," *Sensors*, vol. 18, no. 12, p. 4503, Dec. 2018, doi: [10.3390/s18124503](https://doi.org/10.3390/s18124503).
- [4] A. O. Fernández, C. A. O. Pinatti, R. M. Peris, and N. Laguarda-Miró, "Freeze-damage detection in lemons using electrochemical impedance spectroscopy," *Sensors*, vol. 19, no. 18, p. 4051, Sep. 2019, doi: [10.3390/s19184051](https://doi.org/10.3390/s19184051).
- [5] M. El-Otmami, A. Ait-Oubahou, and L. Zacarías, "Citrus spp.: Orange, mandarin, tangerine, clementine, grapefruit, pomelo, lemon and lime," in *Postharvest Biology and Technology of Tropical and Subtropical Fruits*, Woodhead Publishing Series in Food Science, Technology and Nutrition, E. M. Yahia, Ed. Sawston, U.K.: Woodhead Publishing, 2011, pp. 437–516, doi: [10.1533/9780857092762.437](https://doi.org/10.1533/9780857092762.437).
- [6] H. Zabihi, I. Vogeler, Z. M. Amin, and B. R. Gourabi, "Mapping the sensitivity of citrus crops to freeze stress using a geographical information system in Ramsar, Iran," *Weather Climate Extremes*, vol. 14, pp. 17–23, Dec. 2016.
- [7] US Department of Agriculture, Agricultural Research Service. *FoodData Central*. Accessed: May 20, 2020. [Online]. Available: <https://fdc.nal.usda.gov/fdc-app.html#/food-details/169105/nutrients>
- [8] F. Artes and F. Artes-Hernandez, "Daños por frío en la postrecolección de frutas y hortalizas," in *Avances en Ciencias y Técnicas del Frío*, A. L. Gómez, F. A. Calero, A. Esnoz, and A. E. Nicuesa, Eds. Cartagena, Spain: Univ. Politécnica de Cartagena, 2003, pp. 299–310.
- [9] L. Martínez, A. Ibacache, and L. Rojas, "Daños por heladas en frutales," *Tierra Adentro*, vol. 80, pp. 32–35, May/June 2008.
- [10] R. L. Snyder, J. P. Melo-Abreu, and J. M. Villar-Mir, *Protección Contra Las Heladas: Fundamentos, Práctica y Economía*. Rome, Italy: Food and Agriculture Organization, 2010, p. 78.
- [11] C. Y. Wang, "Chilling and freezing injury," in *The Commercial Storage of Fruits, Vegetables, and Florist and Nursery Stocks*, K. C. Gross, C. Y. Wang, and M. Saltveir, Eds. Washington, DC, USA: USDA, 2016, p. 792.
- [12] V. U. Vallejo, "Daños por heladas en frutales. Sintomatología y evaluación," in *Curs de Valoració de Danys Climatològics i Incendis*. Barcelona, Spain: Centre de Formació i Estudis Agrorurals; Generalitat de Catalunya-Departament d'Agricultura, Alimentació i Acció Rural, 2007.
- [13] G. A. Gonzalez-Aguilar, L. Zacarias, M. Mulas, and M. T. Lafuente, "Temperature and duration of water dips influence chilling injury, decay and polyamine content in 'fortune' mandarins," *Postharvest Biol. Technol.*, vol. 12, pp. 61–69, Aug. 1997, doi: [10.1016/S0925-5214\(97\)00036-7](https://doi.org/10.1016/S0925-5214(97)00036-7).
- [14] J. M. Sala and M. T. Lafuente, "Catalase in the heat-induced chilling tolerance of cold-stored hybrid fortune mandarin fruits," *J. Agricult. Food Chem.*, vol. 47, no. 6, pp. 2410–2414, Jun. 1999, doi: [10.1021/jf980805e](https://doi.org/10.1021/jf980805e).
- [15] M. Rehman, Z. Singh, and T. Khurshid, "Methyl jasmonate alleviates chilling injury and regulates fruit quality in 'midknight' Valencia orange," *Postharvest Biol. Technol.*, vol. 141, pp. 58–62, Jul. 2018, doi: [10.1016/j.postharvbio.2018.03.006](https://doi.org/10.1016/j.postharvbio.2018.03.006).
- [16] G. E. Brown, "Identification of diseases, peel injuries and blemishes of Florida fresh citrus fruit," Florida Dept. Citrus CREC, Lake Alfred, FL, USA, Tech. Rep., 1998, p. 36.
- [17] M. Ruiz-Altisent *et al.*, "Sensors for product characterization and quality of specialty crops—A review," *Comput. Electron. Agr.*, vol. 74, pp. 176–194, Nov. 2010, doi: [10.1016/j.compag.2010.07.002](https://doi.org/10.1016/j.compag.2010.07.002).
- [18] P. K. Jha, E. Xanthakis, S. Chevallier, V. Jury, and A. Le-Bail, "Assessment of freeze damage in fruits and vegetables," *Food. Res. Int.*, vol. 121, pp. 479–496, Jul. 2019, doi: [10.1016/j.foodres.2018.12.002](https://doi.org/10.1016/j.foodres.2018.12.002).
- [19] *Arizona-California Citrus Loss Adjustment Standards Handbook*, USDA, Washington, DC, USA, 1999, p. 41.
- [20] T. T. Hutton and R. H. Cubbedge, "Separation of frozen grapefruit by using emulsions of differing specific gravities," *Proc. Florida State Horticultural Soc.*, vol. 91, pp. 126–128, Jun. 1978.
- [21] W. M. Miller, W. F. Wardowski, and W. Grierson, "Separation and grading of freeze-damaged fruit," in *Fresh Citrus Fruits*, W. F. Wardowski, W. M. Miller, D. J. Hall, and W. Grierson, Eds. Longboat Key, FL, USA: Florida Science Source, 2006, pp. 299–306.
- [22] S. Moomkesh, S. A. Mireei, M. Sadeghi, and M. Nazeri, "Early detection of freezing damage in sweet lemons using vis/SWNIR spectroscopy," *Biosyst. Eng.*, vol. 164, pp. 157–170, Dec. 2017, doi: [10.1016/j.biosystemseng.2017.10.009](https://doi.org/10.1016/j.biosystemseng.2017.10.009).
- [23] E. S. Tan, D. C. Slaughter, and J. F. Thompson, "Freeze damage detection in oranges using gas sensors," *Postharvest Biol. Technol.*, vol. 35, no. 2, pp. 177–182, Feb. 2005, doi: [10.1016/j.postharvbio.2004.07.008](https://doi.org/10.1016/j.postharvbio.2004.07.008).
- [24] D. M. Obenland, L. H. Aung, D. L. Bridges, and B. E. Mackey, "Volatile emissions of navel oranges as predictors of freeze damage," *J. Agricult. Food Chem.*, vol. 51, no. 11, pp. 3367–3371, May 2003, doi: [10.1021/jf021109o](https://doi.org/10.1021/jf021109o).
- [25] D. C. Slaughter, D. M. Obenland, J. F. Thompson, M. L. Arpaia, and D. A. Margosan, "Non-destructive freeze damage detection in oranges using machine vision and ultraviolet fluorescence," *Postharvest Biol. Technol.*, vol. 48, no. 3, pp. 341–346, Jun. 2008, doi: [10.1016/j.postharvbio.2007.09.012](https://doi.org/10.1016/j.postharvbio.2007.09.012).
- [26] P. N. Gambhir, Y. J. Choi, D. C. Slaughter, J. F. Thompson, and M. J. McCarthy, "Proton spin-spin relaxation time of peel and flesh of navel orange varieties exposed to freezing temperature," *J. Sci. Food Agricult.*, vol. 85, no. 14, pp. 2482–2486, 2005.
- [27] A. Fuentes, R. Masot, I. Fernández-Segovia, M. Ruiz-Rico, M. Alcañiz, and J. M. Barat, "Differentiation between fresh and frozen-thawed sea bream (*Sparus aurata*) using impedance spectroscopy techniques," *Innov. Food Sci. Emerg. Technol.*, vol. 19, pp. 210–217, Jul. 2013, doi: [10.1016/j.ifset.2013.05.001](https://doi.org/10.1016/j.ifset.2013.05.001).
- [28] C. Conesa, E. García-Breijo, E. Loeff, L. Seguí, P. Fito, and N. Laguarda-Miró, "An electrochemical impedance spectroscopy-based technique to identify and quantify fermentable sugars in pineapple waste valorization for bioethanol production," *Sensors*, vol. 15, no. 9, pp. 22941–22955, Sep. 2015, doi: [10.3390/s150922941](https://doi.org/10.3390/s150922941).
- [29] J. R. Macdonald and E. Barsoukov, *Impedance Spectroscopy: Theory, Experiment and Applications*, 2nd ed. Hoboken, NJ, USA: Wiley, 2005, p. 616.
- [30] M. Grossi and B. Riccò, "Electrical impedance spectroscopy (EIS) for biological analysis and food characterization: A review," *J. Sensors Sensor Syst.*, vol. 6, no. 2, pp. 303–325, Aug. 2017, doi: [10.5194/jsss-6-303-2017](https://doi.org/10.5194/jsss-6-303-2017).
- [31] A. Fuentes, J. L. Vázquez-Gutiérrez, M. B. Pérez-Gago, E. Vonasek, N. Nitin, and D. M. Barrett, "Application of nondestructive impedance spectroscopy to determination of the effect of temperature on potato microstructure and texture," *J. Food Eng.*, vol. 133, pp. 16–22, Jul. 2014, doi: [10.1016/j.jfoodeng.2014.02.016](https://doi.org/10.1016/j.jfoodeng.2014.02.016).
- [32] Y. Ando, Y. Maeda, K. Mizutani, N. Wakatsuki, S. Hagiwara, and H. Nabetani, "Impact of blanching and freeze-thaw pretreatment on drying rate of carrot roots in relation to changes in cell membrane function and cell wall structure," *LWT Food Sci. Technol.*, vol. 71, pp. 40–46, Sep. 2016, doi: [10.1016/j.lwt.2016.03.019](https://doi.org/10.1016/j.lwt.2016.03.019).
- [33] Y. Ando, Y. Maeda, K. Mizutani, N. Wakatsuki, S. Hagiwara, and H. Nabetani, "Effect of air-dehydration pretreatment before freezing on the electrical impedance characteristics and texture of carrots," *J. Food Eng.*, vol. 169, pp. 114–121, Jan. 2016, doi: [10.1016/j.jfoodeng.2015.08.026](https://doi.org/10.1016/j.jfoodeng.2015.08.026).
- [34] L. Wu, Y. Ogawa, and A. Tagawa, "Electrical impedance spectroscopy analysis of eggplant pulp and effects of drying and freezing-thawing treatments on its impedance characteristics," *J. Food Eng.*, vol. 87, no. 2, pp. 274–280, Jul. 2008, doi: [10.1016/j.jfoodeng.2007.12.003](https://doi.org/10.1016/j.jfoodeng.2007.12.003).
- [35] J. Benavente, J. R. Ramos-Barrado, and A. Heredia, "A study of the electrical behaviour of isolated tomato cuticular membranes and cutin by impedance spectroscopy measurements," *Colloids Surf. A, Physicochem. Eng. Aspects*, vol. 140, nos. 1–3, pp. 333–338, Sep. 1998.
- [36] A. D. Bauchot, F. R. Harker, and W. M. Arnold, "The use of electrical impedance spectroscopy to assess the physiological condition of kiwifruit," *Postharvest Biol. Technol.*, vol. 18, no. 1, pp. 9–18, Jan. 2000.
- [37] A. Chowdhury, T. K. Bera, D. Ghoshal, and B. Chakraborty, "Electrical impedance variations in banana ripening: An analytical study with electrical impedance spectroscopy," *J. Food Process Eng.*, vol. 40, pp. 1–14, Apr. 2017, doi: [10.1111/jfpe.12387](https://doi.org/10.1111/jfpe.12387).

- [38] A. F. Neto, N. C. Olivier, E. R. Cordeiro, and H. P. de Oliveira, "Determination of mango ripening degree by electrical impedance spectroscopy," *Comput. Electron. Agricult.*, vol. 143, pp. 222–226, Dec. 2017, doi: [10.1016/j.compag.2017.10.018](https://doi.org/10.1016/j.compag.2017.10.018).
- [39] Y. Yang, Z.-Y. Wang, Q. Ding, L. Huang, C. Wang, and D.-Z. Zhu, "Moisture content prediction of porcine meat by bioelectrical impedance spectroscopy," *Math. Comput. Model.*, vol. 58, pp. 819–825, Aug. 2013, doi: [10.1016/j.mcm.2012.12.020](https://doi.org/10.1016/j.mcm.2012.12.020).
- [40] J. L. Damez, S. Clerjon, S. Abouelkaram, and J. Lepetit, "Beef meat electrical impedance spectroscopy and anisotropy sensing for non-invasive early assessment of meat ageing," *J. Food Eng.*, vol. 85, pp. 116–122, Mar. 2008, doi: [10.1016/j.jfoodeng.2007.07.026](https://doi.org/10.1016/j.jfoodeng.2007.07.026).
- [41] G. Scandurra, G. Tripodi, and A. Verzera, "Impedance spectroscopy for rapid determination of honey floral origin," *J. Food Eng.*, vol. 119, no. 4, pp. 738–743, Dec. 2013, doi: [10.1016/j.jfoodeng.2013.06.042](https://doi.org/10.1016/j.jfoodeng.2013.06.042).
- [42] N. M'Hiri, D. Veys-Renaux, E. Rocca, I. Ioannou, N. M. Bourdinova, and M. Ghoul, "Corrosion inhibition of carbon steel in acidic medium by orange peel extract and its main antioxidant compounds," *Corrosion Sci.*, vol. 102, pp. 55–62, Jan. 2016, doi: [10.1016/j.corsci.2015.09.017](https://doi.org/10.1016/j.corsci.2015.09.017).
- [43] C. Conesa, J. I. Civera, L. Seguí, P. Fito, and N. Laguarda-Miró, "An electrochemical impedance spectroscopy system for monitoring pineapple waste saccharification," *Sensors*, vol. 16, no. 2, p. 188, Feb. 2016, doi: [10.3390/s16020188](https://doi.org/10.3390/s16020188).
- [44] C. Conesa, L. G. Sánchez, L. Seguí, P. Fito, and N. Laguarda-Miró, "Ethanol quantification in pineapple waste by an electrochemical impedance spectroscopy-based system and artificial neural networks," *Chemometric Intell. Lab. Syst.*, vol. 161, pp. 1–7, Feb. 2017, doi: [10.1016/j.chemolab.2016.12.005](https://doi.org/10.1016/j.chemolab.2016.12.005).
- [45] J. F. MacGregor, M. J. Bruwer, I. Miletic, M. Cardin, and Z. Liu, "Latent variable models and big data in the process industries," *IFAC-PapersOnLine*, vol. 48, no. 8, pp. 520–524, 2015, doi: [10.1016/j.ifacol.2015.09.020](https://doi.org/10.1016/j.ifacol.2015.09.020).
- [46] P. Martínez Gil, N. Laguarda-Miró, J. S. Camino, and R. M. Peris, "Glyphosate detection with ammonium nitrate and humic acids as potential interfering substances by pulsed voltammetry technique," *Talanta*, vol. 115, pp. 702–705, Oct. 2013, doi: [10.1016/j.talanta.2013.06.030](https://doi.org/10.1016/j.talanta.2013.06.030).
- [47] C. Ulrich, H. Petersson, H. Sundgren, F. Björefors, and C. Krantz-Rülcker, "Simultaneous estimation of soot and diesel contamination in engine oil using electrochemical impedance spectroscopy," *Sens. Actuators B, Chem.*, vol. 127, no. 2, pp. 613–618, Nov. 2007, doi: [10.1016/j.snb.2007.05.014](https://doi.org/10.1016/j.snb.2007.05.014).
- [48] C. A. Olivati, A. Riul, D. T. Balogh, O. N. Oliveira, and M. Ferreira, "Detection of phenolic compounds using impedance spectroscopy measurements," *Bioprocess Biosyst. Eng.*, vol. 32, no. 1, pp. 41–46, Jan. 2009, doi: [10.1007/s00449-008-0218-4](https://doi.org/10.1007/s00449-008-0218-4).
- [49] Ł. Górski, W. Sordoń, F. Ciepłia, W. W. Kubiak, and M. Jakubowska, "Voltammetric classification of ciders with PLS-DA," *Talanta*, vol. 146, pp. 231–236, Jan. 2016, doi: [10.1016/j.talanta.2015.08.027](https://doi.org/10.1016/j.talanta.2015.08.027).
- [50] E. G. Breijo, C. O. Pinatti, R. M. Peris, M. A. Fillol, R. Martínez-Máñez, and J. S. Camino, "TNT detection using a voltammetric electronic tongue based on neural networks," *Sens. Actuators A, Phys.*, vol. 192, pp. 1–8, Apr. 2013, doi: [10.1016/j.sna.2012.11.038](https://doi.org/10.1016/j.sna.2012.11.038).
- [51] C. Conesa, L. Seguí, N. Laguarda-Miró, and P. Fito, "Microwaves as a pretreatment for enhancing enzymatic hydrolysis of pineapple industrial waste for bioethanol production," *Food Bioprocess Technol.*, vol. 100, pp. 203–213, Oct. 2016, doi: [10.1016/j.fbp.2016.07.001](https://doi.org/10.1016/j.fbp.2016.07.001).
- [52] S. Rajasekaran and G. A. V. Pai, *Neural Networks, Fuzzy Logic and Genetic Algorithms: Synthesis and Applications*. New Delhi, India: Prentice-Hall, 2004, p. 436.
- [53] T. Kasuba, "Simplified fuzzy ARTMAP," *AI Expert*, vol. 8, no. 11, pp. 18–25, Nov. 1993.
- [54] E. Garcia-Breijo *et al.*, "A comparison study of pattern recognition algorithms implemented on a microcontroller for use in an electronic tongue for monitoring drinking waters," *Sens. Actuators A, Phys.*, vol. 172, no. 2, pp. 570–582, Dec. 2011, doi: [10.1016/j.sna.2011.09.039](https://doi.org/10.1016/j.sna.2011.09.039).
- [55] G. Kumar and R. G. Buchheit, "Use of artificial neural network models to predict coated component life from short-term electrochemical impedance spectroscopy measurements," *Corrosion*, vol. 64, no. 3, pp. 241–254, Mar. 2008, doi: [10.5006/1.3278469](https://doi.org/10.5006/1.3278469).
- [56] A. Eddahech, O. Briat, N. Bertrand, J.-Y. Delétage, and J.-M. Vinassa, "Behavior and state-of-health monitoring of Li-ion batteries using impedance spectroscopy and recurrent neural networks," *Int. J. Electr. Power Energy Syst.*, vol. 42, no. 1, pp. 487–494, Nov. 2012, doi: [10.1016/j.ijepes.2012.04.050](https://doi.org/10.1016/j.ijepes.2012.04.050).
- [57] E. Garcia-Breijo, J. Garrigues, L. Sanchez, and N. Laguarda-Miro, "An embedded simplified fuzzy ARTMAP implemented on a microcontroller for food classification," *Sensors*, vol. 13, no. 8, pp. 10418–10429, Aug. 2013, doi: [10.3390/s130810418](https://doi.org/10.3390/s130810418).
- [58] A. Lasia, *Electrochemical Impedance Spectroscopy and Its Applications*, Springer, Ed. New York, NY, USA, 2014, p. 384, doi: [10.1007/0-306-46916-2_2](https://doi.org/10.1007/0-306-46916-2_2).
- [59] M. Rehman, B. A. J. A. A. Izneid, M. Z. Abdullah, and M. R. Arshad, "Assessment of quality of fruits using impedance spectroscopy," *Int. J. Food Sci. Technol.*, vol. 46, no. 6, pp. 1303–1309, May 2011, doi: [10.1111/j.1365-2621.2011.02636.x](https://doi.org/10.1111/j.1365-2621.2011.02636.x).
- [60] J. Juansah, I. W. Budiastira, K. Dahlan, and K. B. Seminar, "Electrical behavior of garut citrus fruits during ripening changes in resistance and capacitance models of internal fruits," *IJET-IJENS*, vol. 12, no. 4, pp. 1–8, Aug. 2012.
- [61] Y. Ando, K. Mizutani, and N. Wakatsuki, "Electrical impedance analysis of potato tissues during drying," *J. Food Eng.*, vol. 121, pp. 24–31, Jan. 2014, doi: [10.1016/j.jfoodeng.2013.08.008](https://doi.org/10.1016/j.jfoodeng.2013.08.008).
- [62] Y. Ando, S. Hagiwara, and H. Nabetani, "Thermal inactivation kinetics of pectin methylesterase and the impact of thermal treatment on the texture, electrical impedance characteristics and cell wall structure of Japanese radish (*Raphanus Sativus L.*)," *J. Food Eng.*, vol. 199, pp. 9–18, Apr. 2017, doi: [10.1016/j.jfoodeng.2016.12.001](https://doi.org/10.1016/j.jfoodeng.2016.12.001).
- [63] T. Imaizumi, F. Tanaka, D. Hamanaka, Y. Sato, and T. Uchino, "Effects of hot water treatment on electrical properties, cell membrane structure and texture of potato tubers," *J. Food Eng.*, vol. 162, pp. 56–62, Oct. 2015, doi: [10.1016/j.jfoodeng.2015.04.003](https://doi.org/10.1016/j.jfoodeng.2015.04.003).
- [64] T.-H. Chen *et al.*, "Classification of chicken muscle with different freeze-thaw cycles using impedance and physicochemical properties," *J. Food Eng.*, vol. 196, pp. 94–100, Mar. 2017, doi: [10.1016/j.jfoodeng.2016.10.003](https://doi.org/10.1016/j.jfoodeng.2016.10.003).
- [65] L. F. Lima, A. L. Vieira, H. Mukai, C. M. G. Andrade, and P. R. G. Fernandes, "Electric impedance of aqueous KCl and NaCl solutions: Salt concentration dependence on components of the equivalent electric circuit," *J. Mol. Liquids*, vol. 241, pp. 530–539, Sep. 2017, doi: [10.1016/j.molliq.2017.06.069](https://doi.org/10.1016/j.molliq.2017.06.069).
- [66] T. C. Mills, "Seasonal and exponential smoothing," in *Applied Time Series Analysis*. London, U.K.: Academic, 2019, ch. 9, p. 354, doi: [10.1016/B978-0-12-813117-6.00019-3](https://doi.org/10.1016/B978-0-12-813117-6.00019-3).
- [67] R. Masot *et al.*, "Design of a low-cost non-destructive system for punctual measurements of salt levels in food products using impedance spectroscopy," *Sens. Actuators A, Phys.*, vol. 158, no. 2, pp. 217–223, Mar. 2010, doi: [10.1016/j.sna.2010.01.010](https://doi.org/10.1016/j.sna.2010.01.010).
- [68] S. Wold, M. Sjöström, and L. Eriksson, "PLS-regression: A basic tool of chemometrics," *Chemometric Intell. Lab. Syst.*, vol. 58, no. 2, pp. 109–130, Oct. 2001.
- [69] E. Borrás *et al.*, "Olive oil sensory defects classification with data fusion of instrumental techniques and multivariate analysis (PLS-DA)," *Food Chem.*, vol. 203, pp. 314–322, Jul. 2016, doi: [10.1016/j.foodchem.2016.02.038](https://doi.org/10.1016/j.foodchem.2016.02.038).
- [70] I. Jócsák, G. Végvári, and E. Vozáry, "Electrical impedance measurement on plants: A review with some insights to other fields," *Theor. Exp. Plant Physiol.*, vol. 31, no. 3, pp. 359–375, Aug. 2019, doi: [10.1007/s40626-019-00152-y](https://doi.org/10.1007/s40626-019-00152-y).
- [71] C. Gabriel, S. Gabriel, and E. Corthout, "The dielectric properties of biological tissues: I. Literature survey," *Phys. Med. Biol.*, vol. 41, no. 11, pp. 2231–2249, Nov. 1996, doi: [10.1088/0031-9155/41/11/001](https://doi.org/10.1088/0031-9155/41/11/001).
- [72] H. M. Dastjerdi, R. Soltanzadeh, and H. Rabbani, "Designing and implementing bioimpedance spectroscopy device by measuring impedance in a mouse tissue," *J. Med. Signals Sens.*, vol. 3, pp. 94–187, Jul. 2013, doi: [10.4103/2228-7477.120979](https://doi.org/10.4103/2228-7477.120979).



Pablo Albelda Aparisi received the degree in industrial design engineering from the Universitat Politècnica de València in 2020. His research interests are technological design developments for agrifood safety and postharvest quality control as demonstrated in his initial research career and his final degree project. He is an active Research Fellow at the Universitat Politècnica de València and is nowadays involved in the development of a research line on citrus postharvest quality control by electrochemistry.



Elena Fortes Sánchez received the degree in industrial design engineering from the Universitat Politècnica de València in 2020. She is interested in engineering design for development cooperation projects in non-developed countries. Her initial research career has been focused in food safety processes for these purposes. She is also an active Research Fellow at the Universitat Politècnica de València and nowadays involved in a research line on fruit quality control by electrochemical processes for NGO's projects and cooperation.



Rafael Masot Peris received the dual M.Sc. degree in physics and in electronic engineering from Universitat de València, Spain, in 1991 and 1996, respectively, the Ph.D. degree in knowledge area of electronic technology from the Universitat Politècnica de València (UPV) in 2010. He is a Lecturer with the Electronic Engineering Department, UPV. He is currently teaching aerospace engineering for B.Sc. students and sensors for industrial applications for M.Sc. students. He is a member of Interuniversity Research Institute for Molecular Recognition and Technological Development. His main areas of research interest are physical sensors, design of electronic systems for electrochemical measurements techniques, electrical impedance spectroscopy, and multivariate data analysis.



Laura Contat Rodrigo received the M.Sc. degree in chemistry from the Universitat de València, Spain, in 1995, and the Ph.D. degree in the field of polymeric materials from the Universitat Politècnica de València, Spain, in 2000. She is currently an Assistant Professor with the Universitat Politècnica de València and a member of the Interuniversity Research Institute for Molecular Recognition and Technological Development (IDM), Spain. Her research is focused on the development of chemical sensors based on organic thin film transistors.



Nicolás Laguarda-Miró received the degree in civil engineering and the degree in environmental sciences from the Universitat Politècnica de València (UPV) in 1998 and 2000, respectively, and the Ph.D. degree in 2005. He is an Assistant Professor with the UPV. After combining both environmental studies and working at different Civil Engineering Companies as an Engineer, he became a member of the Interuniversity Research Institute for Molecular Recognition and Technological Development, UPV and nowadays his main areas of interest are environmental control, food quality control, and microelectronics-based sensors applied in these fields.